

On Simplified Mechanical Models for Rocket-Body Divergence and Flutter

Tsukasa OHSHIMA and Yoshihiko SUGIYAMA

Department of Aerospace Engineering, Osaka Prefecture University, Sakai-shi, Japan

E-mail address; ohshima@aero.osakafu-u.ac.jp
sugiyama@aero.osakafu-u.ac.jp

The present paper sheds some light on simplified mechanical models for demonstrating aeroelastic instability of flexible rocket bodies accommodated with a stabilizer fin. The dynamic stability of simplified models is discussed by considering models having three degrees of freedom and four-degrees of freedom. The simplified models consist of massless rigid bars connected together by an elastic spring. Concentrated masses are attached to the bar at its ends and joints. The simplified mechanical models in this paper are designed to discuss the effect of 1) degrees of freedom, 2) mass distribution, 3) stiffness distribution, and 4) location of the stabilizer fin on the body instability.

1. NOMENCLATURE

$C_{L\alpha}$: lift curve slope
k	: coefficient of restoring moment
l	: length of rigid bar
l_F	: location of stabilizer fin apart from tail end
L	: aerodynamic load
M	: concentrated mass
S	: reference area of bar
T	: kinetic energy
t	: time
U	: flight velocity
u	: dimensionless flight velocity
V	: potential energy
x, y	: coordinates
α	: angle of attack
ε	: dimensionless location of the stabilizer fin apart from tail end
ϕ	: inclination of bar to horizontal axis
κ	: dimensionless spring constant
μ	: ratio of fluid mass to concentrated mass
ρ	: fluid density
τ	: dimensionless time
ξ, η	: dimensionless coordinates
$1/2\rho V^2$: dynamic pressure

Subscripts

N	: nose
T	: tail
F	: fin

2. INTRODUCTION

Aerospace structures, being extremely light-weighted and thus inevitably very flexible, are prone to dynamic instability under aerodynamic loads. So far a lot of comprehensive textbooks on aeroelasticity has been published; Bisplinghoff, Ashley and Halfman^[1] (1955), Bisplinghoff and Ashley^[2] (1962), Fung^[3] (1969). Recent development of supersonic aircraft and high-performance missiles has presented many new aeroelastic problems. This situation has resulted in a modern course in aeroelasticity; Dowell^[4] (editor, 1989).

The present space age has revealed a new topic of aeroelasticity of rocket-vehicle; Sarafin^[5] (1995). Structural bending and dynamic stability of slender rocket may lead to structural failure and/or trajectory errors. In place of aircraft wing divergence and flutter, rocket-body divergence and flutter are to be discussed in the present context.

Ikeda^[6] (1959) studied dynamic stability of rocket bodies due to aerodynamic loads by discussing a mechanical model having three degrees of freedom (3DOF). He concluded that only rocket-body divergence could take place. Tomita^[7] (1994) investigated a failure of small test rocket vehicle to conclude that the failure of the rocket was attributable to rocket-body divergence. Kobayashi^[8] (1995) conducted experiments of a model space plane to suggest that space planes may be susceptible to body flutter. Under these circumstances, it has raised some questions whether 3DOF mechanical model by Ikeda is suitable for discussing rocket body instability, and whether rocket bodies are susceptible only to divergence, but not to flutter. Thus it is needed to

discuss what are the smallest but sufficient degrees of freedom for the simplified mechanical model of rocket vehicle, and what is the suitable simplified model for studying rocket-body instability. The intended aim of the paper is to discuss simplified mechanical models, which is suitable to grasp a perspective of body divergence and flutter of slender rocket vehicles.

3. STATEMENT OF THE PROBLEM

3-1. Aerodynamic loads

It is assumed that aerodynamic loads are concentrated loads which act on the rocket body at its nose, tail and stabilizer fin. Aerodynamic loads on other portion except at the nose, the tail and on the fin, are negligible, since it is assumed that they are small enough relative to those at the nose, the tail, and on the fin. A fluid flows through the bars at a constant velocity U . The density is denoted by ρ . The aerodynamic loads can be written by

$$\begin{aligned} L_N &= \alpha_N C_{LaN} \frac{1}{2} \rho U^2 S, \\ L_T &= \alpha_T C_{LaT} \frac{1}{2} \rho U^2 S, \\ L_F &= \alpha_F C_{LaF} \frac{1}{2} \rho U^2 S, \end{aligned} \quad (1)$$

where α means the angle of attack, and C_{La} is a lift curve slope. Each subscripts N , T and F express the nose, the tail and the stabilizer fin of the rocket body.

3-2. 3DOF model

Figure 1 shows the simplified model having three degrees of freedom (3DOF). It is assumed that simplified model of a flexible rocket body is accommodated with a stabilizer fin. The model is composed of two rigid bars and one massless elastic joint. Each bar has length l . The joint has the restoring moment coefficient k . The damping of the elastic spring is neglected. The stabilizer fin is attached to the bar l_F apart from the tail.

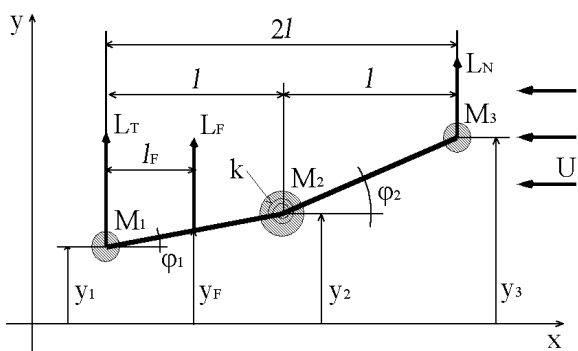


Fig.1 Simplified mechanical model having three degrees of freedom; 3DOF model.

The dimensionless location of the stabilizer fin ε is given by

$$\varepsilon = \frac{l_F}{l}. \quad (2)$$

Concentrated masses M_i ($i=1,2,3$) are attached to each bar at both ends. The modeling process of mass distribution is illustrated in Figure 2.

The mass ratio β is given by

$$\begin{aligned} \frac{M_2}{M_1} &= 1 + \beta, \\ \frac{M_3}{M_1} &= \beta. \end{aligned} \quad (3)$$

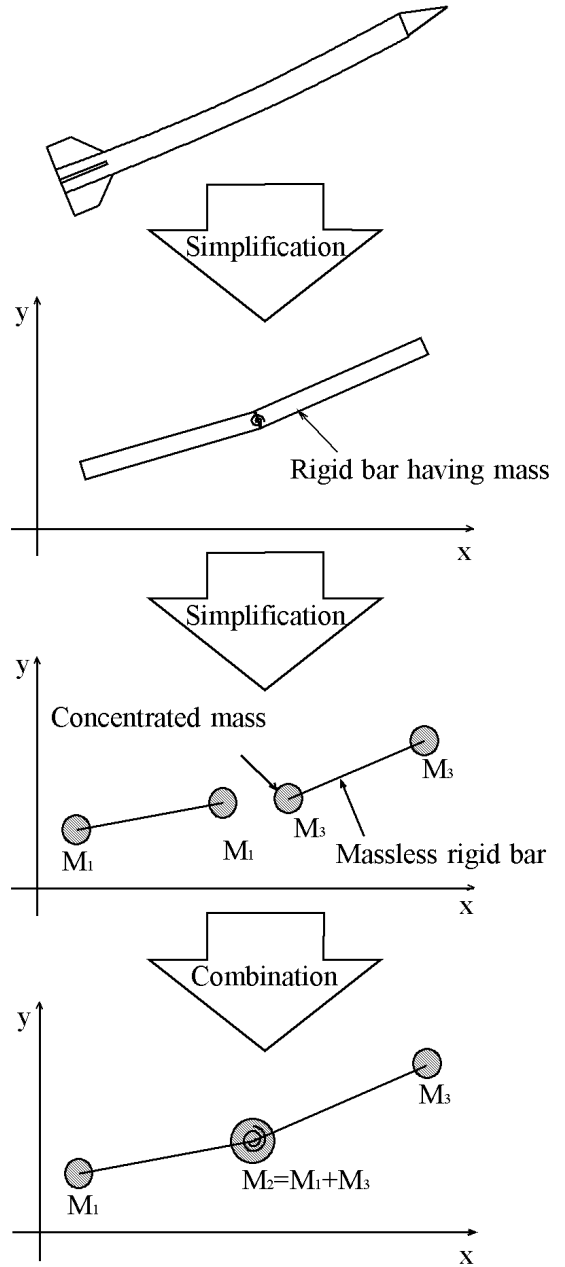


Fig.2 Modeling of mass distribution.

Inclination of each bar to the horizontal axis is expressed by

$$\begin{aligned}\phi_1 &= \frac{y_2 - y_1}{l}, \\ \phi_2 &= \frac{y_3 - y_2}{l},\end{aligned}\quad (4)$$

where y_i ($i = 1, 2, 3$) are the displacements of the rocket body.

The angles of attack can be given by

$$\begin{aligned}\alpha_N &= \phi_2 - \frac{1}{U} \frac{dy_3}{dt}, \\ \alpha_T &= \phi_1 - \frac{1}{U} \frac{dy_1}{dt}, \\ \alpha_F &= \phi_1 - \frac{1}{U} \left\{ (1-\varepsilon) \frac{dy_1}{dt} + \varepsilon \frac{dy_2}{dt} \right\}, \quad \text{for } 0 \leq \varepsilon < 1 \\ \alpha_F &= \phi_2 - \frac{1}{U} \left\{ (2-\varepsilon) \frac{dy_2}{dt} + (\varepsilon-1) \frac{dy_3}{dt} \right\}. \quad \text{for } 1 < \varepsilon \leq 2\end{aligned}\quad (5)$$

It is noted that the effect of the rigid body motion of the models on aerodynamic load are taken into account. This means that aerodynamic damping is taken into account in stability analysis.

3-3. 4DOF model

Figure 3 shows a simplified model having four degrees of freedom (4DOF). The model is composed of three rigid bars and two massless elastic joints. Each bar has length l . Each joint has the restoring moment coefficients k_1, k_2 , respectively. The restoring spring ratio is given by

$$\kappa = \frac{k_2}{k_1}. \quad (6)$$

A stabilizer fin is attached to the bar l_F apart from the tail. The dimensionless fin location ε is given by the same form as Eq. (2).

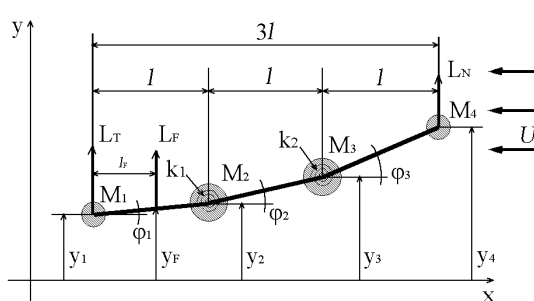


Fig.3 Simplified mechanical model having four degrees of freedom: 4DOF model.

Concentrated masses M_i ($i = 1, 2, 3, 4$) are attached to each bar at its both ends. The mass ratio β_i ($i = 1, 2$) is given by

$$\begin{aligned}\frac{M_2}{M_1} &= 1 + \beta_1, & \frac{M_3}{M_1} &= \beta_1 + \beta_2, \\ \frac{M_4}{M_1} &= \beta_2, & \frac{M}{M_1} &= \beta_1.\end{aligned}\quad (7)$$

where M is a half of the assumed total mass of the second bar.

Inclination of each bar to the horizontal axis is expressed by

$$\begin{aligned}\phi_1 &= \frac{y_2 - y_1}{l}, \\ \phi_2 &= \frac{y_3 - y_2}{l}, \\ \phi_3 &= \frac{y_4 - y_3}{l},\end{aligned}\quad (8)$$

where y_i ($i = 1, 2, 3, 4$) are the displacements of the slender body.

The angles of attack can be given by

$$\begin{aligned}\alpha_N &= \phi_3 - \frac{1}{U} \frac{dy_3}{dt}, \\ \alpha_T &= \phi_1 - \frac{1}{U} \frac{dy_1}{dt}, \\ \alpha_F &= \phi_1 - \frac{1}{U} \left\{ (1-\varepsilon) \frac{dy_1}{dt} + \varepsilon \frac{dy_2}{dt} \right\}, \quad \text{for } 0 \leq \varepsilon < 1 \\ \alpha_F &= \phi_2 - \frac{1}{U} \left\{ (2-\varepsilon) \frac{dy_2}{dt} + (\varepsilon-1) \frac{dy_3}{dt} \right\}, \quad \text{for } 1 < \varepsilon < 2 \\ \alpha_F &= \phi_3 - \frac{1}{U} \left\{ (3-\varepsilon) \frac{dy_3}{dt} + (\varepsilon-2) \frac{dy_4}{dt} \right\}. \quad \text{for } 2 < \varepsilon \leq 3\end{aligned}\quad (9)$$

4. EQUATIONS OF MOTION

4-1. Basic equations for 3DOF model

Lagrangian equations of motion are written in the form

$$\frac{d}{dt} \left(\frac{\partial T}{\partial \dot{y}_n} \right) - \frac{\partial T}{\partial y_n} + \frac{\partial V}{\partial y_n} = Q_n, \quad (n = 1, 2, 3) \quad (10)$$

where T is a kinetic energy, V is a potential energy, and Q_n are external generalized forces.

The kinetic energy of the 3DOF model is expressed by

$$T = \frac{1}{2} M_1 \dot{y}_1^2 + \frac{1}{2} M_2 \dot{y}_2^2 + \frac{1}{2} M_3 \dot{y}_3^2. \quad (11)$$

The potential energy of the model is given by

$$V = \frac{1}{2} k (\phi_2 - \phi_1)^2. \quad (12)$$

The external generalized forces are given in the form

$$\begin{aligned} Q_1 &= L_T + (1-\varepsilon)L_F, \quad Q_2 = \varepsilon L_F, \\ Q_3 &= L_N, \\ &\text{for } 0 \leq \varepsilon < 1 \end{aligned} \quad (13-1)$$

$$\begin{aligned} Q_1 &= L_T, \quad Q_2 = (2-\varepsilon)L_F, \\ Q_3 &= (\varepsilon-1)L_F + L_N, \\ &\text{for } 1 \leq \varepsilon < 2 \end{aligned} \quad (13-2)$$

Substitution of Eqs.(1)~(5), (11), (12), (13) to Eq.(10) leads the equations for a small motion of the 3DOF model in the dimensionless forms;

$$\begin{aligned} &\frac{d^2\eta_1}{d\tau^2} + (\eta_1 - 2\eta_2 + \eta_3) \\ &= \frac{C_{LaT}}{2} \mu u^2 \left(\eta_2 - \eta_1 - \frac{1}{u} \frac{d\eta_1}{d\tau} \right) \\ &+ (1-\varepsilon) \frac{C_{LaF}}{2} \mu u^2 \left[\eta_2 - \eta_1 - \frac{1}{u} \left\{ (1-\varepsilon) \frac{d\eta_1}{d\tau} + \varepsilon \frac{d\eta_2}{d\tau} \right\} \right], \\ &(1+\beta) \frac{d^2\eta_2}{d\tau^2} + (-2\eta_1 + 4\eta_2 - 2\eta_3) \\ &= \varepsilon \frac{C_{LaF}}{2} \mu u^2 \left[\eta_2 - \eta_1 - \frac{1}{u} \left\{ (1-\varepsilon) \frac{d\eta_1}{d\tau} + \varepsilon \frac{d\eta_2}{d\tau} \right\} \right], \\ &\beta \frac{d^2\eta_3}{d\tau^2} + (\eta_1 - 2\eta_2 + \eta_3) = \frac{C_{LaN}}{2} \mu u^2 \left(\eta_3 - \eta_2 - \frac{1}{u} \frac{d\eta_3}{d\tau} \right), \\ &\text{for } 0 \leq \varepsilon < 1 \end{aligned} \quad (14-1)$$

$$\begin{aligned} &\frac{d^2\eta_1}{d\tau^2} + (\eta_1 - 2\eta_2 + \eta_3) \\ &= \frac{C_{LaT}}{2} \mu u^2 \left(\eta_2 - \eta_1 - \frac{1}{u} \frac{d\eta_1}{d\tau} \right), \\ &(1+\beta) \frac{d^2\eta_2}{d\tau^2} + (-2\eta_1 + 4\eta_2 - 2\eta_3) = \\ &(2-\varepsilon) \frac{C_{LaF}}{2} \mu u^2 \left[\eta_3 - \eta_2 - \frac{1}{u} \left\{ (2-\varepsilon) \frac{d\eta_2}{d\tau} + (\varepsilon-1) \frac{d\eta_3}{d\tau} \right\} \right], \\ &\beta \frac{d^2\eta_3}{d\tau^2} + (\eta_1 - 2\eta_2 + \eta_3) \\ &= \frac{C_{LaN}}{2} \mu u^2 \left(\eta_3 - \eta_2 - \frac{1}{u} \frac{d\eta_3}{d\tau} \right) \\ &+ (\varepsilon-1) \frac{C_{LaF}}{2} \mu u^2 \left[\eta_3 - \eta_2 - \frac{1}{u} \left\{ (2-\varepsilon) \frac{d\eta_2}{d\tau} + (\varepsilon-1) \frac{d\eta_3}{d\tau} \right\} \right], \\ &\text{for } 1 < \varepsilon \leq 2 \end{aligned} \quad (14-2)$$

where the dimensionless parameters are as follows;

$$\begin{aligned} \eta_n &= \frac{y_n}{l}, \quad (n=1,2,3) \\ u &= \sqrt{\frac{M_1}{k}} U, \\ \mu &= \frac{\rho Sl}{M_1}, \\ \tau &= \frac{1}{l} \sqrt{\frac{k}{m}} t. \end{aligned} \quad (15)$$

The solution to Eqs.(14) is now cast in the form

$$y_n = Y_n e^{\lambda t}, \quad (n=1,2,3). \quad (16)$$

Substituting Eq.(16) into Eqs.(14), one obtains the characteristic equation

$$\lambda^2(a_1\lambda^4 + a_2\lambda^3 + a_3\lambda^2 + a_4\lambda + a_5) = 0 \quad (17)$$

The root of Eq.(17) may be expressed by a complex eigen-value

$$\lambda = \sigma \pm i\omega, \quad (18)$$

where σ is a real part, ω is a imaginary part, and i is the imaginary unit.

The system is stable when $\sigma < 0$. The system is dynamically unstable (flutter) when $\sigma > 0$ and $\omega \neq 0$, while it is statically unstable (divergence) when $\sigma > 0$ and $\omega = 0$.

The boundary of dynamic instability (body-flutter) is determined by the Routh-Hurwitz condition

$$a_2 a_3 a_4 - a_1 a_4^2 - a_2^2 a_5 = 0. \quad (19)$$

The limit for static instability (body-divergence) is determined by the condition of vanishing characteristic root

$$a_5 = 0. \quad (20)$$

4-2. Basic equations for 4DOF model

The kinetic energy of the 4DOF model is expressed by

$$T = \frac{1}{2} M_1 \dot{y}_1^2 + \frac{1}{2} M_2 \dot{y}_2^2 + \frac{1}{2} M_3 \dot{y}_3^2 + \frac{1}{2} M_4 \dot{y}_4^2 \quad (21)$$

The potential energy of this system is given by

$$V = \frac{1}{2} k_1 (\phi_2 - \phi_1)^2 + \frac{1}{2} k_2 (\phi_3 - \phi_2)^2 \quad (22)$$

The external generalized forces are given in the form

$$Q_1 = L_T + (1-\varepsilon)L_F, \quad Q_2 = \varepsilon L_F,$$

$$Q_3 = 0, \quad Q_4 = L_N,$$

$$\text{for } 0 \leq \varepsilon < 1 \quad (23-1)$$

$$Q_1 = L_T, \quad Q_2 = (2-\varepsilon)L_F,$$

$$Q_3 = (\varepsilon-1)L_F, \quad Q_4 = L_N,$$

$$\text{for } 1 < \varepsilon < 2 \quad (23-2)$$

$$Q_1 = L_T, \quad Q_2 = 0,$$

$$Q_3 = (3-\varepsilon)L_F, \quad Q_4 = (\varepsilon-2)L_F + L_N.$$

$$\text{for } 2 < \varepsilon \leq 3 \quad (23-3)$$

Substituting Eqs.(1),(2),(6),(7),(8),(9),(21),(22),(23) into Eq.(10), one obtains the equations for a small motion of the 4DOF model in the dimensionless forms;

$$\begin{aligned} &\frac{d^2\eta_1}{d\tau^2} + (\eta_1 - 2\eta_2 + \eta_3) \\ &= \frac{C_{LaT}}{2} \mu u^2 \left(\eta_2 - \eta_1 - \frac{1}{u} \frac{d\eta_1}{d\tau} \right) \\ &+ (1-\varepsilon) \frac{C_{LaF}}{2} \mu u^2 \left[\eta_2 - \eta_1 - \frac{1}{u} \left\{ (1-\varepsilon) \frac{d\eta_1}{d\tau} + \varepsilon \frac{d\eta_2}{d\tau} \right\} \right], \end{aligned}$$

$$\begin{aligned}
& (1 + \beta_1) \frac{d^2 \eta_2}{d\tau^2} + (-2\eta_1 + 4\eta_2 - 2\eta_3) + \kappa(\eta_2 - 2\eta_3 + \eta_4) \\
& = \varepsilon \frac{C_{LaF}}{2} \mu u^2 \left[\eta_2 - \eta_1 - \frac{1}{u} \left\{ (1 - \varepsilon) \frac{d\eta_1}{d\tau} + \varepsilon \frac{d\eta_2}{d\tau} \right\} \right], \\
& (\beta_1 + \beta_2) \frac{d^2 \eta_3}{d\tau^2} \\
& + (\eta_1 - 2\eta_2 + \eta_3) + \kappa(-2\eta_2 + 4\eta_3 - 2\eta_4) = 0, \\
& \beta_2 \frac{d^2 \eta_4}{d\tau^2} + \kappa(\eta_2 - 2\eta_3 + \eta_4) \\
& = \frac{C_{LaN}}{2} \mu u^2 (\eta_4 - \eta_3 - \frac{1}{u} \frac{d\eta_4}{d\tau}), \\
& \text{for } 0 \leq \varepsilon < 1 \quad (24-1)
\end{aligned}$$

$$\begin{aligned}
& \frac{d^2 \eta_1}{d\tau^2} + (\eta_1 - 2\eta_2 + \eta_3) \\
& = \frac{C_{Lat}}{2} \mu u^2 (\eta_2 - \eta_1 - \frac{1}{u} \frac{d\eta_1}{d\tau}), \\
& (1 + \beta_1) \frac{d^2 \eta_2}{d\tau^2} + (-2\eta_1 + 4\eta_2 - 2\eta_3) + \kappa(\eta_2 - 2\eta_3 + \eta_4) \\
& = (2 - \varepsilon) \frac{C_{LaF}}{2} \mu u^2 \left[\eta_3 - \eta_2 - \frac{1}{u} \left\{ (2 - \varepsilon) \frac{d\eta_2}{d\tau} + \varepsilon \frac{d\eta_3}{d\tau} \right\} \right], \\
& (\beta_1 + \beta_2) \frac{d^2 \eta_3}{d\tau^2} \\
& + (\eta_1 - 2\eta_2 + \eta_3) + \kappa(-2\eta_2 + 4\eta_3 - 2\eta_4) \\
& = (\varepsilon - 1) \frac{C_{LaF}}{2} \mu u^2 \left[\eta_3 - \eta_2 - \frac{1}{u} \left\{ (2 - \varepsilon) \frac{d\eta_2}{d\tau} + \varepsilon \frac{d\eta_3}{d\tau} \right\} \right], \\
& \beta_2 \frac{d^2 \eta_4}{d\tau^2} + \kappa(\eta_2 - 2\eta_3 + \eta_4) \\
& = \frac{C_{LaN}}{2} \mu u^2 (\eta_4 - \eta_3 - \frac{1}{u} \frac{d\eta_4}{d\tau}), \\
& \text{for } 1 < \varepsilon < 2 \quad (24-2)
\end{aligned}$$

$$\begin{aligned}
& \frac{d^2 \eta_1}{d\tau^2} + (\eta_1 - 2\eta_2 + \eta_3) \\
& = \frac{C_{Lat}}{2} \mu u^2 (\eta_2 - \eta_1 - \frac{1}{u} \frac{d\eta_1}{d\tau}), \\
& (1 + \beta_1) \frac{d^2 \eta_2}{d\tau^2} \\
& + (-2\eta_1 + 4\eta_2 - 2\eta_3) + \kappa(\eta_2 - 2\eta_3 + \eta_4) = 0, \\
& (\beta_1 + \beta_2) \frac{d^2 \eta_3}{d\tau^2} \\
& + (\eta_1 - 2\eta_2 + \eta_3) + \kappa(-2\eta_2 + 4\eta_3 - 2\eta_4) \\
& = (3 - \varepsilon) \frac{C_{LaF}}{2} \mu u^2 \left[\eta_4 - \eta_3 - \frac{1}{u} \left\{ (3 - \varepsilon) \frac{d\eta_3}{d\tau} + (\varepsilon - 2) \frac{d\eta_4}{d\tau} \right\} \right], \\
& \beta_2 \frac{d^2 \eta_4}{d\tau^2} + \kappa(\eta_2 - 2\eta_3 + \eta_4) \\
& = \frac{C_{LaN}}{2} \mu u^2 (\eta_4 - \eta_3 - \frac{1}{u} \frac{d\eta_4}{d\tau}) \\
& + (\varepsilon - 2) \frac{C_{LaF}}{2} \mu u^2 \left[\eta_4 - \eta_3 - \frac{1}{u} \left\{ (3 - \varepsilon) \frac{d\eta_3}{d\tau} + (\varepsilon - 2) \frac{d\eta_4}{d\tau} \right\} \right], \\
& \text{for } 2 \leq \varepsilon < 3 \quad (24-3)
\end{aligned}$$

with dimensionless parameters

$$\begin{aligned}
\eta_n &= \frac{y_n}{l}, \quad (n=1,2,3,4) \\
u &= \sqrt{\frac{M_1}{k_1}} U, \\
\mu &= \frac{\rho S l}{M_1}, \\
\tau &= \frac{1}{l} \sqrt{\frac{k_1}{m}} t. \quad (25)
\end{aligned}$$

The solution to Eqs. (24) is now put in the form

$$y_n = Y_n e^{\lambda \tau}, \quad (n=1,2,3,4). \quad (26)$$

Substituting Eq.(26) into Eqs.(24), one obtains the characteristic equation

$$\lambda^2 (a_1 \lambda^6 + a_2 \lambda^5 + a_3 \lambda^4 + a_4 \lambda^3 + a_5 \lambda^2 + a_6 \lambda + a_7) = 0 \quad (27)$$

The root of Eq.(27) may be expressed by a complex eigen-value as shown in Eq.(18)

The boundary of dynamic instability (body-flutter) is determined by the Routh-Hurwitz condition.

The limit for static instability (body-divergence) is determined by the condition of vanishing characteristic root

$$a_7 = 0. \quad (28)$$

5. RESULTS AND DISCUSSIONS

Effect of degrees of freedom

Figure 4 shows the dimensionless critical flight velocity u_{cr} as a function of the dimensionless location of the stabilizer fin ε for the 3DOF model. It is confirmed that the 3DOF model loses its stability only by divergence. Figure 5 shows the same stability map for the 4DOF model. The 4DOF model, however, implies that the body flutter may take place in addition to the body divergence, if the stabilizer fin is fixed to the rocket body ahead of the tail end. It is suggested that a simplified mechanical model for aeroelasticity of rocket body should have 4DOF.

Effect of mass distribution

Figure 6 shows the dimensionless critical flight velocity u_{cr} as a function of the mass ratio β_2 for the 4DOF model with $C_{LaN} = 2.0$, $C_{Lat} = 4.0$, $\mu = 0.002$, and $\beta_1 = 1.0$. It is assumed here that a typical rocket is not accommodated with a stabilizer fin in order to discuss the effect of a mass distribution. This system loses its stability only through divergence. The critical velocity increases as the mass ratio increases. Thus a rocket accommodated with heavy a payload may be stabilizing.

Effect of stiffness distribution

Figure 7 shows the dimensionless critical flight velocity u_{cr} as a function of the restoring spring ratio κ for the 4DOF model with $C_{LoN}=2.0$, $C_{Lat}=4.0$, $\mu=0.002$, and $\beta_1=1.0$. This system loses the stability only through divergence. The critical velocity increases as the restoring moment coefficient increases. Thus the low stiffness at the nose part of rocket body may be destabilizing.

Effect of location of the stabilizer fin

Figures 8 (a), (b) and (c) show the dimensionless critical flight velocity u_{cr} as a function of the dimensionless location of the stabilizer fin ε for the 4DOF model with $C_{LoN}=2.0$, $C_{Lat}=4.0$, $C_{LoF}=4.0$, $\mu=0.002$, $\beta_1=1.0$ and $\beta_2=1.0$. Fig.8 (a) shows the effect of the fin when it is fixed on the first bar, while Figs.8 (b) and (c) demonstrate the effect when it is mounted on the second and third bar, respectively. The rocket body loses its stability by divergence in the range of $0 \leq \varepsilon \leq 2.26$. However, flutter type instability can take place in the range of $2.26 < \varepsilon \leq 3.0$. Thus it is confirmed that a stabilizer fin attached closer to the tail may be stabilizing. The stabilizer fin at the nose may result in destabilization.

6. CONCLUDING REMARKS

The effect of degrees of freedom as well as mass distribution, stiffness distribution and the location of a stabilizer fin on the stability of simplified mechanical model has been discussed. The following conclusions can be drawn;

- 1) Simplified mechanical model should have at least 4DOF in investigating aeroelasticity of rocket bodies.

2) As to the effect of mass distribution and stiffness distribution, it has been found by stability analysis that the instability of the mechanical models is of divergence-type, regardless the different values of the dimensionless mass ratio β and the dimensionless spring constant κ .

3) A stabilizer fin near at the tail may be effective in stabilizing the rocket body.

REFERENCES

- [1] Bisplinghoff, R. L., Ashley, H., and Halfman, R. L., 1955, *Aeroelasticity*, Addison-Wesley Publishing Company, Cambridge, Mass.
- [2] Bisplinghoff, R. L., and Ashley, H., 1962, *Principles of Aeroelasticity*, John Wiley and Sons, INC, New York.
- [3] Y.C.Fung., 1969, *An Introduction to The Theory of Aeroelasticity*, Dover Publication, INC, New York.
- [4] Dowell, E. H. et al., 1978, *A Modern Course in Aeroelasticity*, Kluwer Academic Publishers, Dordrecht, The Netherlands, Chap.3.
- [5] Sarafim, T. P., 1995, *Spacecraft Structures and Mechanisms from Conzept to Launch*, Kluwer Academic Publishers, Dordrecht, The Netherlands.
- [6] Ikeda, K., 1959, "Approximate Analysis of Body Flutter of Rockets (Second Report)," *Journal of the Japan Society of Aeronautical Engineering*, Vol.7-70, pp.265 -269.
- [7] Tomita, N., 1994, "A Study of Body Divergence of a Small Rocket (1st report: Theory and Flight Date Analysis)," *Trans. JSME, Series C*, Vol. 60-580, pp.59-66.
- [8] Kobayashi, S. 1995, "Low Speed Wind Tunnel Test for Body Flutter," *Proceedings of the JSASS/JSME Structures Conference*, Vol.37, pp. 85-88.

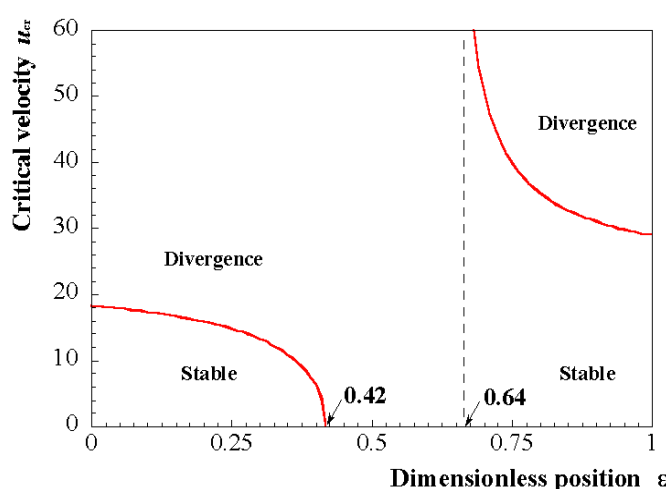


Fig.4 Effect of fin location on stability (3DOF model)

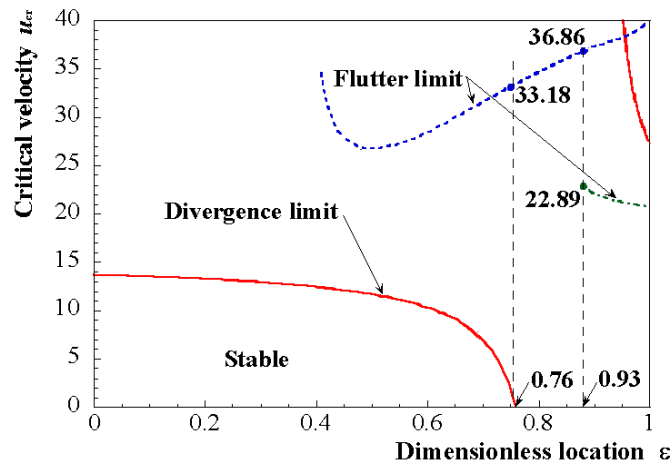


Fig.5 Effect of fin location on stability (4DOF model)
 $(C_{L\alpha N}=2, C_{L\alpha i}=0, C_{L\alpha f}=4, \mu=0.002, \beta_1=1)$

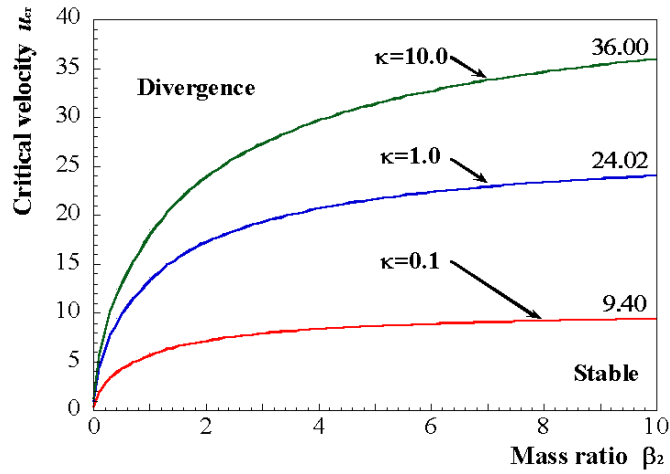


Fig.6 Effect of mass distribution on stability (4DOF model)
 $(C_{L\alpha N}=2, C_{L\alpha i}=4, C_{L\alpha f}=0, \mu=0.002, \beta_1=1)$

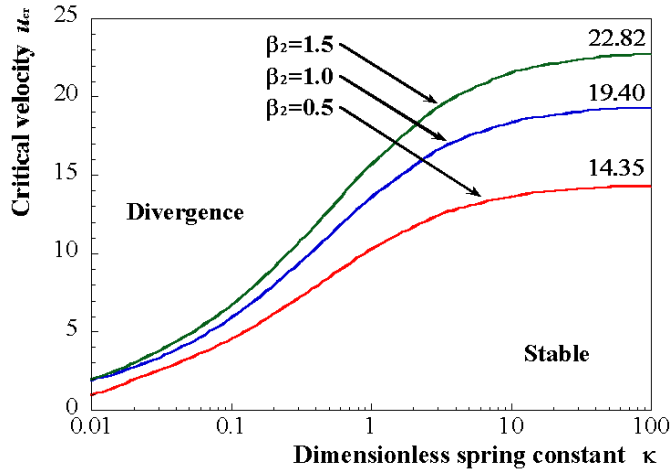


Fig.7 Effect of stiffness distribution on stability (4DOF model)
 $(C_{L\alpha N}=2, C_{L\alpha i}=4, C_{L\alpha f}=0, \mu=0.002, \beta_1=1)$

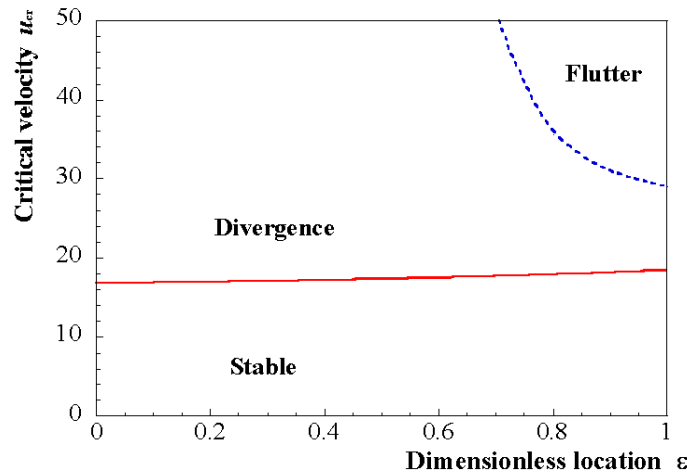


Fig.8(a) Effect of fin location on stability (4DOF model)
 $(C_{L\alpha N}=2, C_{L\alpha T}=4, C_{L\alpha f}=4, \mu=0.002, \beta_1=1)$

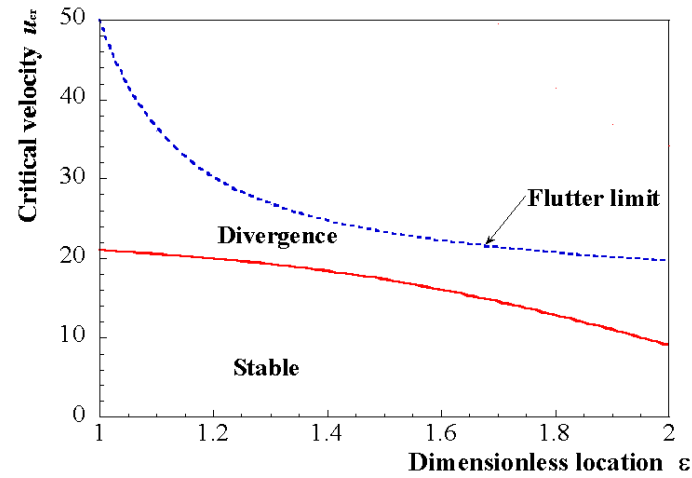


Fig.8(b) Effect of fin location on stability (4DOF model)
 $(C_{L\alpha N}=2, C_{L\alpha T}=4, C_{L\alpha f}=4, \mu=0.002, \beta_1=1)$

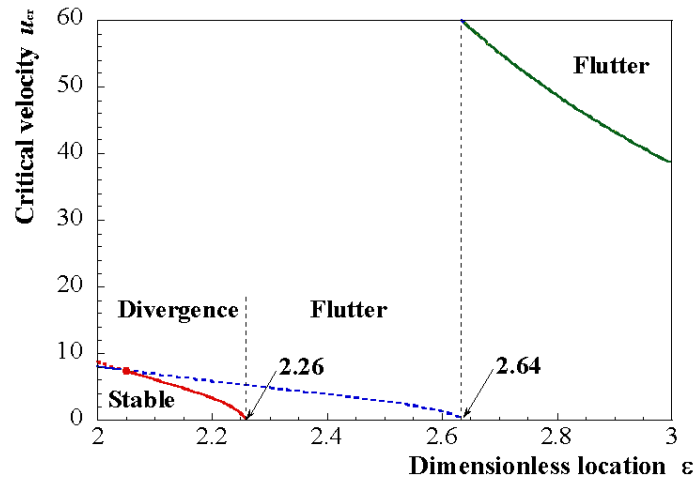


Fig.8(c) Effect of fin location on stability (4DOF model)
 $(C_{L\alpha N}=2, C_{L\alpha T}=4, C_{L\alpha f}=4, \mu=0.002, \beta_1=1)$